JOURNAL OF GEOPHYSICAL RESEARCH, VOL. 91, NO. A3, PAGES 3106–3116, MARCH 1, 1986

On the Correlation of Whistlers and Associated Subionospheric VLF/LF Perturbations

U. S. INAN AND D. L. CARPENTER

STAR Laboratory, Stanford University, Stanford, California

Several periods of whistler-associated subionospheric signal perturbations (i.e., Trimpi events) observed at Palmer, Antarctica ($L \sim 2.4$) have been studied. In a case study of the time signature of the signal perturbations during a 10-min recording period on March 30, 1983, the time delay between the whistler-producing spheric and the onset of the change was found to be in the range 0.52-0.62 s, independent of the amplitude of the change. Event amplitude, as expected from previous work, was found to be well correlated with the associated whistler wave intensity. Other temporal features such as the rise and decay times of the perturbations were also found to be independent of the event amplitude. These results are consistent with a recent theoretical model of gyroresonant particle scattering interaction in the magnetosphere. The amplitudes of simultaneous perturbations on signals of different frequency and arrival bearing were well correlated in several cases, but exhibited case to case differences that appear to depend upon the spatial distribution of precipitation regions. Whistler occurrence times during two recording periods were found to approximately obey a Poisson distribution, while the statistics of Trimpi event occurrence in those periods showed significant deviations from Poisson behavior. The probability of random alignment in time of the whistlers subionospheric and perturbations is estimated to be $< 10^{-14}$, in agreement with previous inferences of a cause and effect relation between whistlers and VLF/LF perturbations. Although nearly all of the whistlers observed originated in northern hemisphere lightning, the first example was found of a Trimpi event associated with a southern hemisphere source.

1. INTRODUCTION

The Trimpi effect, involving subionospheric VLF/LF signal amplitude and phase perturbations that occur in correlation with magnetospheric whistlers, has attracted considerable attention in recent years. The observed association of the two phenomena has been attributed to whistler-induced precipitation of bursts of energetic (> 40 keV) electrons from the magnetosphere, resulting in the perturbation of the earth-ionosphere waveguide via localized secondary ionization enhancements in the ionospheric D region [*Helliwell et al.*, 1973; *Lohrey and Kaiser*, 1979].

Recent research on the Trimpi effect has shown that such events can be commonly observed inside the plasmasphere at middle to low latitudes [*Carpenter and LaBelle*, 1982; *Leyser et al.*, 1984] on signals in the VLF, LF and MF frequency ranges (up to $\sim$ 800 kHz) [*Carpenter et al.*, 1984]; observations at higher latitudes near to and outside the plasmapause have also been reported [*Carpenter et al.*, 1985; *Hurren et al.*, 1985]. Trimpi effects have been observed in the northern as well as the southern hemisphere [*Dingle and Carpenter*, 1981; *Kintner and LaBelle*, 1984]. Direct satellite observations of a sequence of precipitating electron pulses in one-to-one correlation with whistlers observed at a ground station have been reported in association with Trimpi events [*Voss et al.*, 1984]. Rocket observations include the simultaneous measurement of an electron precipitation burst and a whistler [*Rycroft*, 1973] and the detection of energetic electrons in time correlation with lightning detected on the ground [*Goldberg et al.*, 1985].

Theoretical work has mostly been limited to modeling of separate aspects of the Trimpi phenomenon such as the whistler-particle interaction [*Chang and Inan*, 1983, 1985] and the effects of localized D region perturbations on subionospheric VLF propagation [*Tolstoy et al.*, 1982]. A first-order interpretative model of a phase Trimpi event, involving the whistler-particle interaction, secondary D region ionization and the resulting subionospheric signal phase perturbation, was recently presented [*Inan et al.*, 1985].

Our purpose in this paper is to provide preliminary experimental answers to a number of questions that have been raised in the course of recent work. One question concerns the statistical relations between the occurrence times of a series of recorded whistlers and the times of a series of observed subionospheric signal perturbations. Ample evidence already exists in the literature in support of a correlation between the two time series, but our study for the first time argues for this connection within a more formal statistical framework. Other questions concern the extent to which temporal features of the perturbations depend upon the intensity of the precipitation burst, as reflected in the perturbation amplitude and the amplitude of the associated whistler. Two case studies as well as additional data provide preliminary answers to questions on these topics, and call attention to the variety of quantities (i.e., degrees of freedom) that are measurable in the case of Trimpi events, especially on multiple signals. Such measurements can potentially be used to extract quantitative information about the whistler-particle interaction, the spatial distribution of precipitation regions and the transient response of the lower ionosphere to bursts of precipitantly energetic electrons.

In the following, we first present the experimental data, with initial emphasis on the correlation of perturbation signatures with the whistler wave intensity. We then discuss the occurrence distribution of whistler-producing spherics and subionospheric signal perturbations. A separate section

Paper number 5A8890.
0148-0227/86/005A-8890$05.00

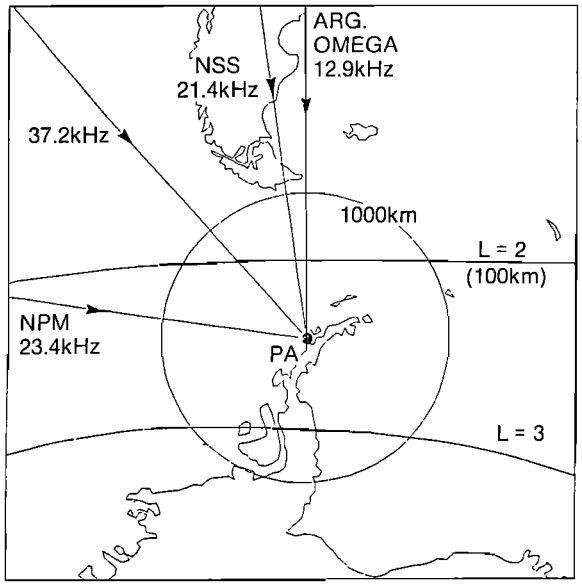

Fig. 1. Map showing examples of great circle paths from various signal sources to Palmer (PA) station, Antarctica.

discusses precipitation induced by a whistler originating in the southern hemisphere, a type seldom observed at Palmer. This is followed by a section of summary and conclusions.

2. Experimental Results

Data Acquisition

The data described here were acquired at Palmer Station, Antarctica (65°S, 64°W, $L \simeq 2.4$), during 1983. The geometry of the observations and sample subionospheric signal paths that were monitored are shown in Figure 1. The locations of the various signal sources and their operating frequencies are given in Table 1.

The data were recorded on eight-channel Sanborn charts and on magnetic tapes. The charts include amplitude records of signals from a number of transmitters, the phase of one signal, and integrated VLF intensity in the frequency bands 0.5–1.0 kHz and 2.0–4.0 kHz. Trimpi events were identified by inspecting the charts for both the characteristic perturbation signatures, illustrated following reprocessing in Figure 2, as well as a time correlation of the events with whistlers which appear as spikes on a record of integrated 2- to 4-kHz VLF amplitude.

The magnetic tapes contain broadband VLF recordings (0–30 kHz) for one 10-min or 12-min period each hour throughout the local night (typically 0150–1000 UT during March/April). Amplitudes of selected transmitter signals were measured using narrowband VLF receivers connected to either one of two separate loop antennas oriented in the magnetic north-south and east-west directions. The receiver outputs (in this case from the north-south antenna) were recorded on a separate tape track as voltage-controlled oscillator (VCO) outputs. In addition, a single VLF phase tracking receiver was used to measure the phase of one selected transmitter signal (12.9-kHz Omega, Argentina, for the cases discussed here), and the output from this receiver was also recorded on the tape as VCO output. A total of fiveVCO channels were available for recording. The data from magnetic tapes were used for measurements of the correlated whistlers and for high-time resolution measurements of the VLF/LF signal phase perturbations.

TABLE 1. List of Transmitters Observed at Palmer Station

Transmitter	Location	Latitude	Longitude	Frequency
NSS	Maryland	39°N	76°W	21.4 kHz
NPM	Hawaii	21°N	158°W	23.4 kHz
LF	California	35°N	117°W	37.2 kHz
Omega	Argentina	43°S	65°W	12.9 kHz

Periods of Analysis

The period selected for the principal case study is 0500–0630 UT on March 30, 1983. During this time, broadband VLF recordings and high time resolution VCO data were available in the 10-min period 0550–0600 UT. For the rest of the period, only chart data were available; thus, while measurements were made of event amplitudes and occurrence, it was not possible to accurately measure temporal features or the causative whistler characteristics. The analysis of the selected period was supplemented by data from a 19-min recording on September 15, 1983, during which both broadband VLF and VCO data were available. Station chart data from several other days were also used to investigate amplitude correlations between pairs of signals.

Some features of the data from this period were reported previously, an example being the wide frequency range, from VLF to MF (800 kHz), of simultaneous perturbations [*Carpenter et al.*, 1984]. The phase perturbations on the Omega,

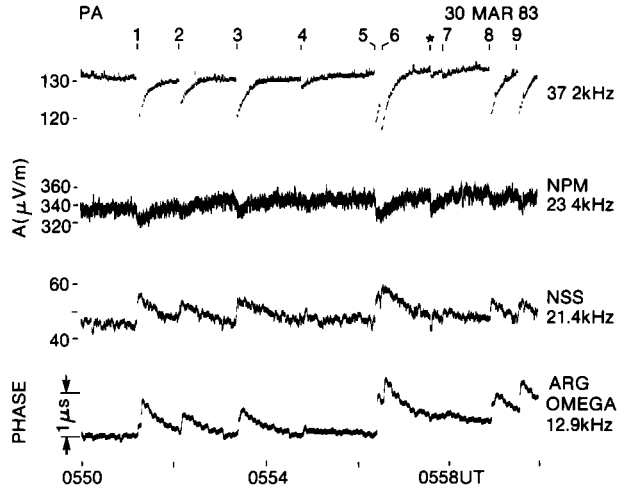

Fig. 2. Amplitudes (linear scales) of 37.2 kHz, NPM, NSS and the phase of the 12.9-kHz Omega, Argentina, signals observed during a 10-min period at Palmer on March 30, 1983. The absolute signal strengths indicated for 37.2 kHz, NPM and NSS are ~42 dB, 34 dB, and 26 dB above the noise level, respectively. The 10 perturbation events observed on 37.2 kHz (with characteristic rapid onset and slow decay) are marked above. The event marked with a star is associated with a two-hop whistler and is separately discussed in section 4. The record was produced by reprocessing VLF narrow-band receiver outputs recorded on magnetic tape as voltage-controlled oscillator (VCO) signals. The sawtooth nature of the phase record is due to the slow drift of the phase holding circuit during the signal-off periods.

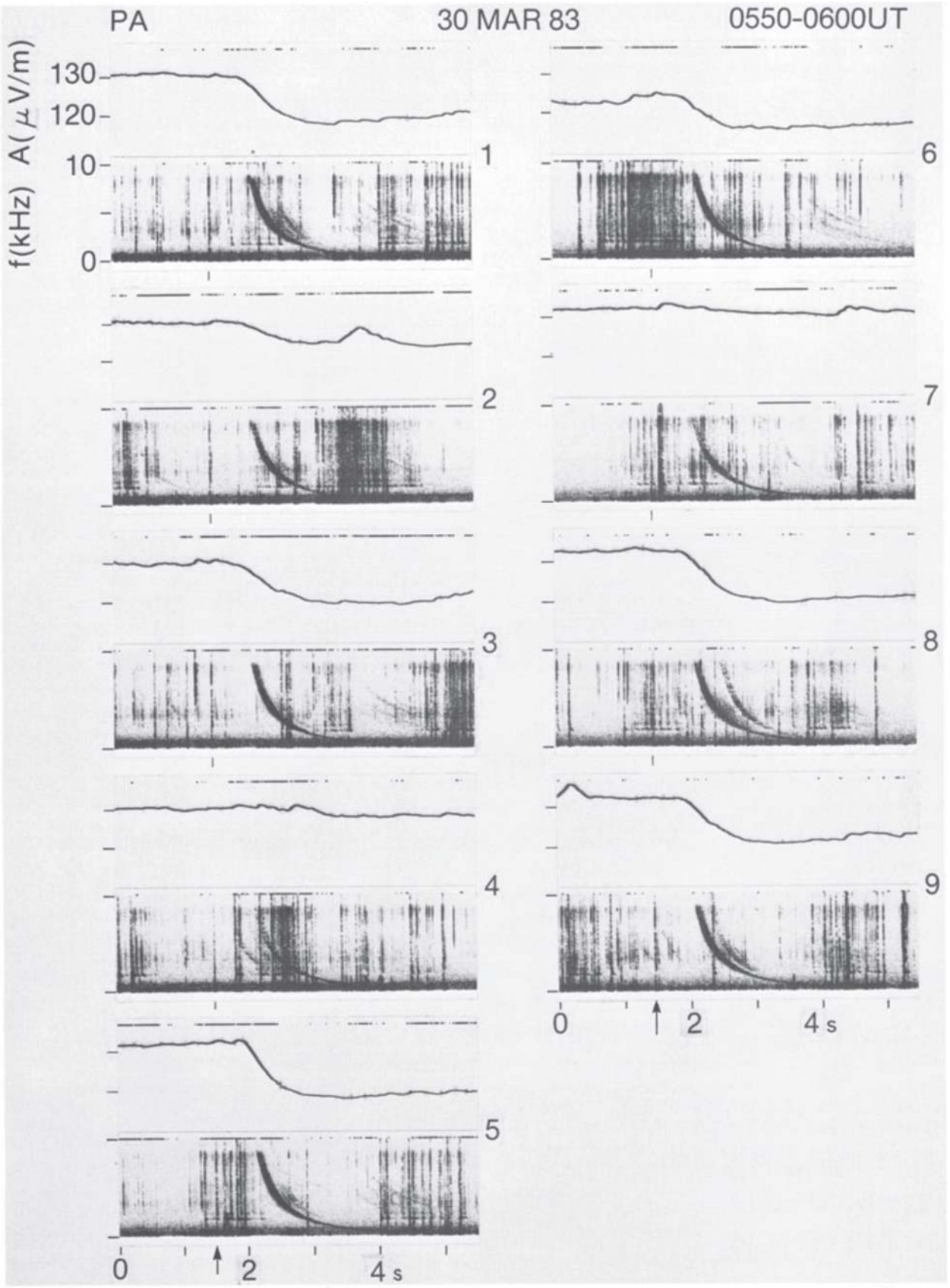

Fig. 3. Correlation of the perturbation events with magnetospheric whistler spectra for events 1–9 identified in Figure 2. The upper panel of each pair represents the 37.2 kHz on a linear scale intensity while the lower panel shows the whistler activity on a 0- to 10-kHz frequency-time display generated at constant signal input level. The time of reception of the whistler-generating spheric is indicated by an arrow or tick mark in the lower margin. Several of the whistlers such as 1 and 5 exhibit multipath fine structure that trail the main component in the ~ 2 to 5-kHz range. One-hop whistlers from other lightning sources appear in several cases, notably 4, 8, and 9. Third-hop echoes of the main component, propagating on several paths, are seen clearly near $t = 8$s in events 3 and 6.

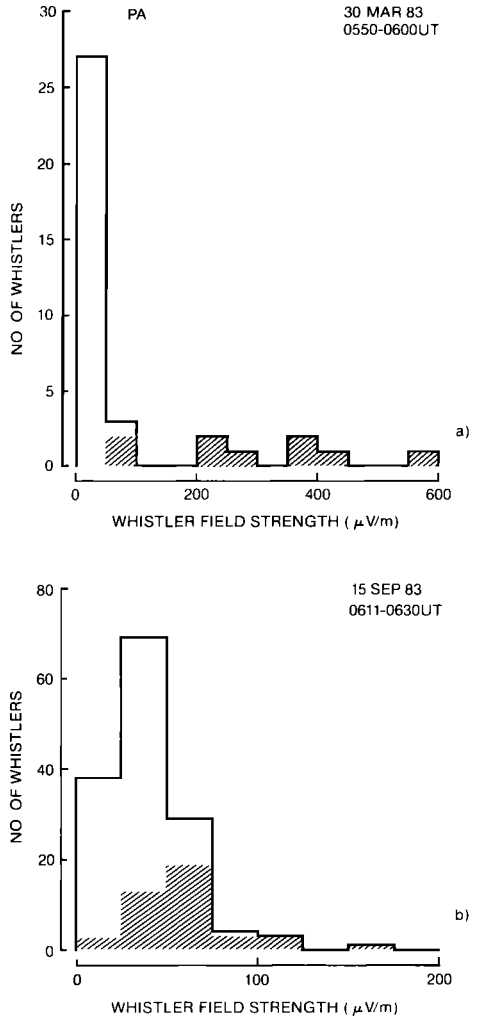

Fig. 4. (*a*) Histogram showing the number of detectable whistlers as a function of whistler field strength observed during 0550–0600 UT on March 30, 1983. The shaded portions indicate whistlers which were associated with a Trimpi event. (*b*) Similar histogram for the period 0611-0630 UT on September 15, 1983.

Argentina, signal were presented in a recent paper in which a first-order theoretical interpretation of an individual phase Trimpi event was developed [*Inan et al.*, 1985].

Examples of Whistler-Associated Perturbations

During the 10-min period of high resolution data, 10 different subionospheric signal perturbation events were observed. These are illustrated in Figure 2 by VCO records of the amplitude of a 37.2-kHz signal, amplitudes of NPM (23.4 kHz) and NSS (21.4 kHz), and the phase of the Omega, Argentina (12.9 kHz), signal. In this context, a perturbation "event" was defined as a $> 1\%$ change in amplitude (on 37.2 kHz) or a $> 0.05^\circ$ phase change, occurring within a time less than a few seconds and followed by a slow, order-of-10 s recovery toward the pre-event level. Of the 10 perturbations, nine are marked as events 1–9 and one is separately identified by a star. In most of the following analysis, we refer to the nine labeled events; the other event was associated with a whistler originating in the southern hemisphere and is separately discussed in section 4 below.

Each of the nine independently identified perturbation events was found to be associated with a magnetospheric whistler, as illustrated in Figure 3, where the upper panels show the VCO records of 37.2-kHz signal amplitude and the lower panels the corresponding 0- to 10-kHz frequency-time spectra. The dispersion of the whistlers indicates that they originated from lightning flashes in the northern hemisphere; the causative atmospherics, as determined from whistler dispersion analysis, were directly identifiable on the records and are indicated by arrows or marks below the spectrograms. These data show the repeatability of the association with whistlers, while also illustrating the variations from one event to another in terms of the size of the amplitude change. The perturbations for events 4 and 7 are almost too small to be noticeable on these expanded records, although they are clearly identifiable on the compressed record of Figure 2, top panel.

Whistler Field Strength

The whistler activity was measured from the broadband VLF data using a frequency tracking filter. The filter was set at a standby frequency of 5 kHz and automatically tracked the frequency variation of signals with intensity at ~ 5 kHz, above a threshold level of ~ 5 μV/m (received on a single loop antenna oriented in the magnetic north south direction). On this basis, 38 whistler events were detected during the 10-min period. The field strength of these whistlers was measured from the output of the tracking filter. For most of the 38 cases, the field intensity peaked at ~ 5 kHz; this peak intensity is used below as the measure of whistler field strength for March 30, 1983.

Figure 4*a* shows a histogram of the field strength distribution of the 38 whistler events. The shaded areas represent those whistlers that were accompanied by a detectable subionospheric signal perturbation. The result indicates that Trimpi events were mainly associated with the stronger

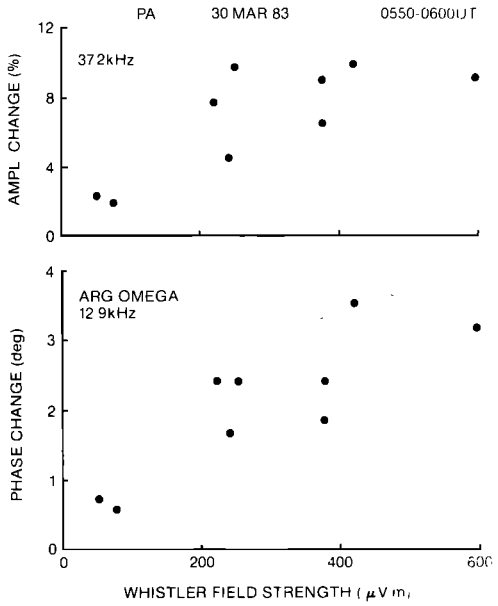

Fig. 5. The percentage amplitude change of the 37.2-kHz signal (top) and the Omega, Argentina, phase charge (bottom) plotted as a function of whistler-associated field strength. The detection threshold for the amplitude changes is $\sim 1\%$ while for the phase changes it is $\sim 0.2^\circ$.

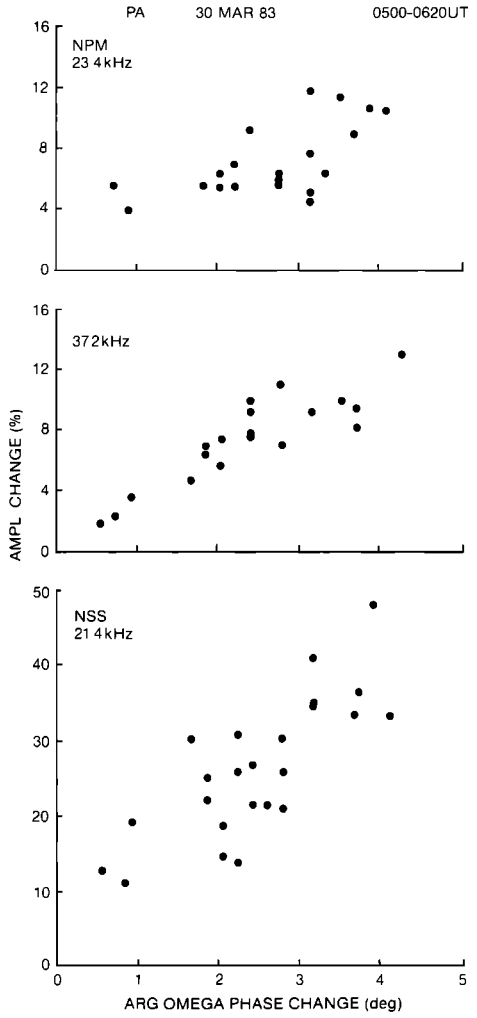

Fig. 6. Correlations of perturbation amplitudes on various signals with the Omega, Argentina, phase changes for the period of Figure 2. Note that the vertical scales are not all the same. Some events were not measurable on all the signals.

observed whistlers, and that nearly all whistlers with amplitude > 50 μV/m produced Trimpi events. The latter result is not always true, for example in cases of multipath propagation in which some of the paths follow field lines that are near the receiver but not near the affected signal path(s) (see, for example, *Carpenter and LaBelle* [1982]).

A larger data set, from September 15, 1983, is illustrated in Figure 4*b*. In this case the whistlers exhibited two principal components instead of one (as on March 30) occurred at higher rates, and were characterized by a more compact amplitude distribution. In a 19-min period, 41 Trimpi events were identified on VCO records and 154 whistlers were detected by the tracker.

Again, Trimpi events tended to be associated with the stronger observed whistlers. Lack of an event with some stronger whistlers and occurrence of events with some weaker ones is attributed to the multipath and hence distributed nature of whistler propagation, as well as the nonuniform manner in which available whistler paths are excited by successive lightning flashes. The association of a few stronger whistlers with Trimpi events may have been obscured by spheric-associated noise on the VCO record.

The relationship between one-hop whistler field strength and the size of the associated subionospheric signal perturbation is illustrated in Figure 5, where the percentage change in the 37.2-kHz amplitude and the phase change of the Omega,Argentina, signal for the nine events of March 30 are plotted against the whistler wave intensity. The figure indicates that the size of the ionospheric perturbation is proportional to the wave intensity. This is consistent with theoretical expectations [*Inan et al.*, 1985], and with results from an earlier case study in which a linear relationship was found for wave intensities above $\sim$ 10 μV/m [*Carpenter and LaBelle*, 1982]. In the case of Figure 5 the data are insufficient for the determination of a threshold wave intensity above which detectable Trimpi events were produced. However, the travel time characteristics of most of the whistlers represented in Figure 4*a* were similar, and hence that figure can be used to infer a threshold (on March 30) of $\sim$ 50 μV/m.

Intercorrelation of Perturbation Size on Different Signals

While broadband VLF data are only available for the 10-min period of 0550-0600 UT, on March 30, measurements of perturbation amplitudes were made from chart data covering the longer period of 0500–0620 UT. Figure 6 shows the

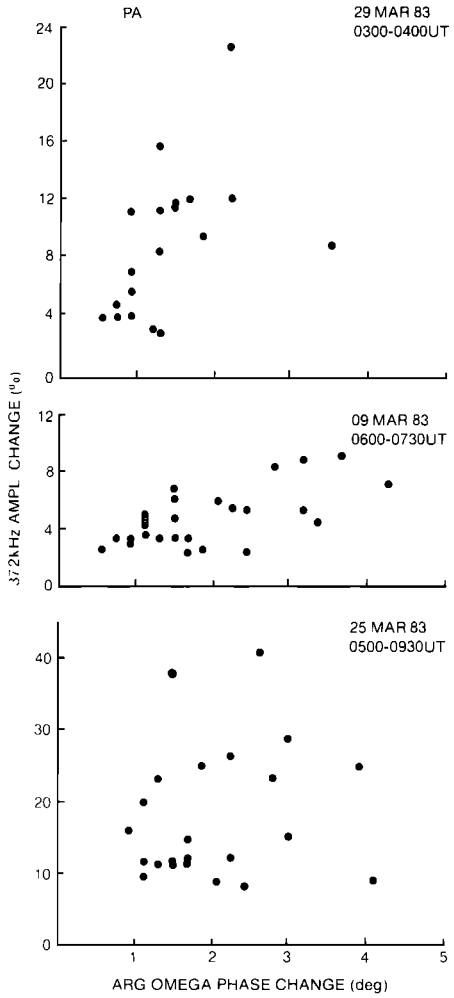

Fig. 7. The relationship between percentage amplitude charge on 37.2 kHz and the Omega, Argentina, phase change for Trimpi events on three different days in March 1983.

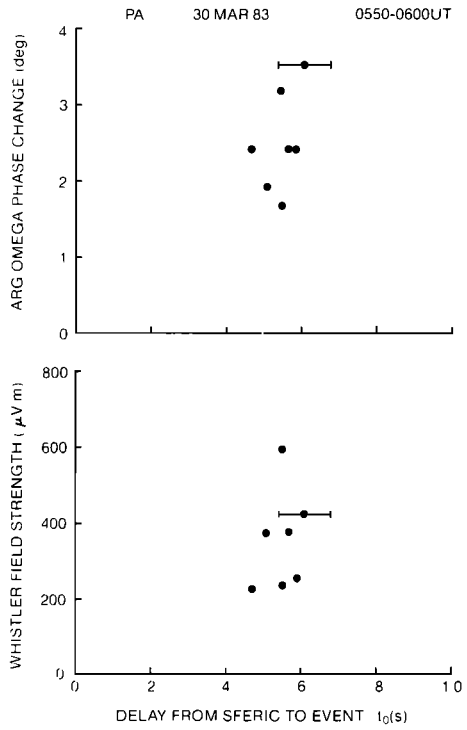

Fig. 8. (Top) The Argentina Omega phase perturbation size and (bottom) associated whistler field strength versus the time delay t_o between the whistler-producing spheric and the perturbation onset (defined as the ~ 10% point). The error bars represent the uncertainty in determining the onset time.

percentage amplitude changes on the NPM, 37.2-kHz, and NSS signals plotted against the phase change of the Omega, Argentina, signal. In general the data show that the perturbation sizes on various signals were well correlated with one another. This suggests that the spatial distribution of precipitation region(s) associated with each whistler did not vary appreciably from one event to another over this time period, at least in the vicinity of the great circle paths from the signal sources to Palmer Station (see Figure 1).

The absolute values of the percentage amplitude perturbations, in this case in the range ~2 to 12% for 37.2 kHz and ~10 to 50% for NSS, can apparently differ widely from signal to signal. These differences probably depend upon the location of the precipitation region(s) with respect to the particular great circle paths. It is known that the amplitude distribution of the subionospheric signal along a given path exhibits relatively sharp maxima and minima [*Watt*, 1967], and calculations have indicated that localized D region perturbations centered near minima should cause larger percentage changes than those near maxima [*Tolstoy*, 1983]. The latitudinal or longitudinal extent of the precipitation regions may also be a controlling factor [*Inan et al.*, 1985].

To further illustrate the cross correlation of perturbations on multiple signals we show in Figure 7 the percentage perturbation size on 37.2 kHz plotted against the phase change on Omega, Argentina, on three other days in March 1983. The variations in slope, say between March 29 and March 9, are believed to represent spatial distributions of the precipitation region(s), that differ in terms of their latitudinal extent and/or in terms of their location with respect to amplitude maxima and minima as discussed above. Differences in the degree of correlation, say between March 25 and March 30 (Figure 6, middle panel) may also reflect the variability in the manner in which energy from successive whistler-causing lightning flashes is distributed among multiple whistler paths. Detailed interpretation of such data will require application of a two-dimensional model of earth-ionosphere waveguide propagation.

Temporal Features

The time signatures of Trimpi events such as those illustrated in Figure 2 are characterized by three parameters, (1) the time delay t_o between the whistler-producing spheric and the onset of the associated subionospheric perturbation (defined as the 10% point), (2) the risetime t_r of the subionospheric perturbation (defined as the time between 10% and 90% points), and (3) the decay time t_d of the perturbation (defined as the time between the postmaximum 90% level and the 10% point). In this subsection we present the measurements of these parameters on the 37.2-kHz signals shown in Figure 2, top panel, and investigate relationships between these and the other measured quantities, such as the perturbation size and the associated whistler field strength.

Figure 8 shows the phase change of the Omega, Argentina, signal and the whistler field intensity versus the onset delay t_o for the seven larger Trimpi events. The measurement error for the delay is mainly due to the identification of the perturbation onset and is indicated with horizontal bars. All the measured delays are seen to lie in the range 0.52–0.62 s, and can be considered equal since the range is comparable to the measurement error. The data illustrate the lack of any clear relationship between the onset delay t_o and the size of the perturbation or the whistler field strength. This is consistent with the supposition that the subionospheric perturbations are caused by whistler-induced precipitation of energetic electrons through gyroresonant scattering; the delay time is then expected to be to first order independent of wave amplitude, and to depend primarily upon the travel time along the field line of the waves and the electrons, which in turn is determined by the path L value, cold plasma density and the whistler frequency range [*Chang and Inan*, 1985].

Figure 9 shows measured values of the rise (t_r) and decay (t_d) times as a function of the size of the Omega, Argentina, phase change. (The Omega signal phase is chosen here due to its being a more directly measured quantity than the whistler field strength that must be defined at a specific frequency. However, also note from Figure 5 that the phase changes are well correlated with whistler field intensity.) The measurement errors are indicated by vertical bars. The determination of the risetime is complicated by the response time of the VCO circuit, which was 200–300 ms. Thus the given t_r values should be viewed as upper limits. The implications of Figure 9 are similar to those of Figure 8, namely that the temporal features are not correlated with the perturbation size.

Both the t_r and t_d are measurable quantities that contain important physical information. It has been suggested that the decay time t_d represents the attachment time of excess electrons to neutrals in the D region [*Dingle*, 1977; *Dingle and Carpenter*, 1981]. Measurements of this parameter should be useful as a diagnostic of the processes governing transient response characteristics of the lower ionosphere. For example, the fact that the decay time on March 30 did

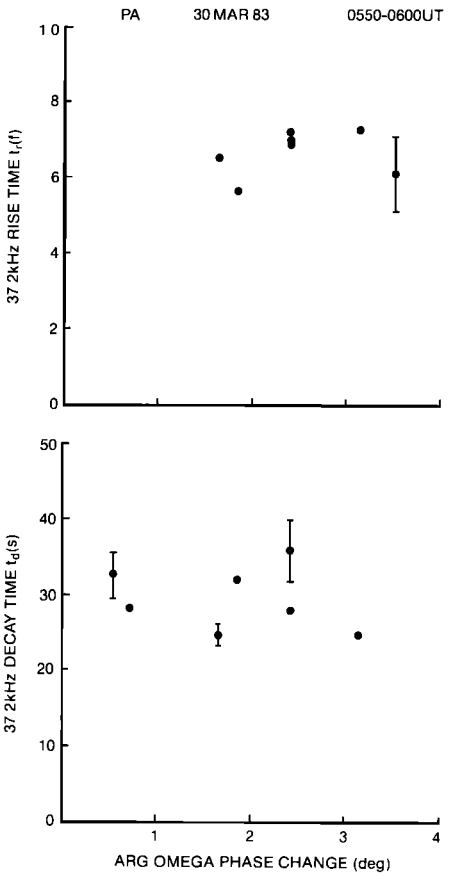

Fig. 9. The rise (t_r) and decay (t_d) times of the 37.2-kHz perturbations on March 30, 1983, plotted against the Omega, Argentina, phase change. Seven of the nine possible events (Figure 2) were measurable in each case.

not vary systematically with event size suggests that attachment was dominant, as opposed to recombination, since in the former case the rate of decrease of electron density is proportional to the density itself, and not density squared, resulting in exponential decay with a fixed time constant [*Bailey*, 1968; *Dingle*, 1977].

The rise time t_r represents the duration of the precipitation burst triggered by the whistler, a quantity determined primarily by (1) the wave and particle travel times along the field line, which in turn depend on L shell and cold plasma density [*Chang and Inan*, 1985], (2) the relative magnitude of the wave-particle scattering coefficients at various latitudes along the field line, and (3) the energetic particle distribution. The particle distribution constitutes a weighting function for contributions to the wave-induced precipitation flux from interactions at different latitudes involving particles of various energies [*Inan et al.*, 1982; *Chang and Inan*, 1985]. In a previous interpretive study of the March 30, 1983 case, the whistler-particle interaction was modeled using a test particle approach, and the duration of the whistler-induced precipitation pulse was estimated to be ~ 0.5 s [*Inan et al.*, 1985], consistent with the measured t_r values given in Figure 9*a*. Accurate measurements of this parameter can be expected to yield information concerning the microphysics of the wave-particle interaction (e.g., the extent of the effective wave-particle interaction region) and/or the energetic particle distribution function. Among the several signals shown in Figure 2, 37.2 kHz was best defined for purposes of measuring the time signature parameters discussed above. However, we note that while most events were simultaneous on all the channels, the rise and decay times tended to differ between signals. For example, the risetimes on NPM and NSS appear to be substantially longer than on 37.2 kHz, and there is some indication of slower decay times on NSS. These variations are not understood, but are believed to represent additional means by which multichannel signals can be used to obtain "images" of precipitation activity. The apparent anomalies may, in part, result from a number of effects such as whistler mode echoing and extended precipitation due to particle backscattering. We note from Figure 3 (and other records not shown) that the March 30 whistlers contain evidence of third-hop echoing as well as multipath fine structure in the first hop.

3. Occurrence Statistics

Thus far we have simply assumed that whistlers and temporally associated signal perturbations were causally related. We now propose to demonstrate this causal relation on statistical grounds. We will consider the occurrence distributions of both whistlers and signal perturbations, and then show that the probability of observing the reported associations (i.e., Trimpi events) would be $< 10^{-14}$ if the whistlers and signal changes were occurring independently.

Occurrence of Whistler-Producing Spherics

During the period of 0550–0600 UT on March 30, 1983, 38 one-hop whistler events were detected using the automatic detection scheme discussed above in connection with Figure 4. This indicates an average occurrence rate of $\lambda \simeq 0.063$ events per second. The "occurrence time" of a given whistler event was taken to be represented by the time of the whistler-producing lightning discharge, which was determined with an accuracy of ~ 10 ms. This definition is convenient, since each whistler wave arrives at the observing site in a dispersed form, covering a time of 1–3 s.

As is the case for most natural random counting processes, the occurrence of whistler-producing lightning discharges might be expected to have a Poisson distribution. To characterize the statistics of spheric distribution during the 10-min period, the interarrival times (i.e., the time intervals between successive events) were measured. A well known property of Poisson processes [*Davenport*, 1970] is

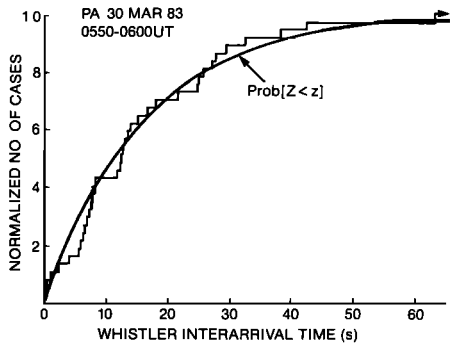

Fig. 10. Whistler occurrence statistics for March 30, 1983, represented by a plot of the normalized number of cases for which the interarrival time (Z) (time between events) was less than a given value (Z). The exponential distribution function (Prob [$Z < z$]) computed from (1) is shown for comparison.

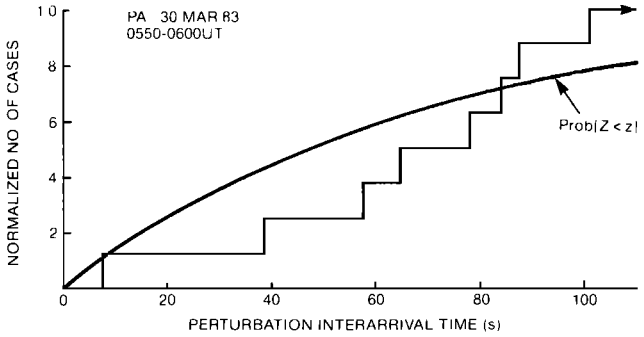

Fig. 11. Occurrence statistics of the nine subionospheric perturbations on March 30, 1983. The format is the same as in Figure 10.

that the interarrival times of event occurrences are governed by an exponential distribution. Thus the probability that interarrival time Z is less than or equal to a given value $z > 0$ is equal to

$$\text{Prob}[Z \leq z] = 1 - e^{-\lambda z} \quad (1)$$

Figure 10 shows the normalized number from a total of 38 cases for which the interarrival time was less than a given value, plotted against time in seconds. Superimposed is the exponential probability distribution computed from (1) above. The comparison indicates that the statistics of the whistler-producing spheric occurrence can be reasonably well represented as a Poisson process. The Poisson nature also implies that successive event occurrences were statistically independent [*Davenport*, 1970].

Occurrence of VLF/LF Perturbations

During the 10-min period of interest on March 30, 10 subionospheric signal perturbation events were detected (see Figure 2). The interarrival times of those numbered 1–9 were measured and are plotted in Figure 11 in the format of Figure 10. Also shown in Figure 11 is the exponential probability distribution computed from (1) using an average event occurrence rate of $\lambda \simeq 0.015$ events per second. On the basis of these relatively crude statistics, we see that the occurrence distribution of subionospheric perturbations deviates substantially from Poisson behavior. This suggests that in this case, the successive subionospheric signal perturbations were not statistically independent. The tendency for events to occur at preferred intervals of $\sim$ 80 s is apparent from the raw data of Figure 2.

In order to obtain better counting statistics for Trimpi event occurrence, we have analyzed data from the period 0611–0630 UT on September 15, 1983. During this period, 154 whistler-producing spherics and 41 subionospheric signal perturbations were observed. Figures 12 and 13 show plots of the measured interarrival time statistics for both processes in the formats of Figures 10 and 11. The comparison confirms the Poisson nature of the whistler activity and again shows a deviation of Trimpi event occurrence from Poisson behavior.

The correlation between perturbation amplitude and associated whistler intensity (Figure 5) suggests that the statistics of stronger whistlers (e.g., $> 50\mu$ V/m) should be similar to that of the subionospheric VLF/LF perturbations. The deviation of both types of events from Poisson behavior suggests that their statistical patterns are due either to the physics of atmospheric lightning, or to a magnetospheric process that quasi-periodically increases the spatial growth rate of whistlers, and hence their particle scattering effects.

Under certain circumstances, a "dead time" effect might occur, such that a relatively strong whistler observed immediately following a Trimpi event produces either no detectable charge or a weak event, thus leading to departure from a Poisson distribution of signal perturbations. An example of this effect was reported by *Carpenter and LaBelle* [1982], but it does not appear to have been important in the present cases, in both of which relatively large events occurred within seconds of previous large perturbations (see Figure 2, events 6 and 7).

The strong whistler events may have originated within a limited area close to the illuminated whistler paths. The data may then have developed a Poisson character only because of the addition of many weaker whistlers, launched by lightning located at greater distances from the paths.

Probability of Coincidental Alignment

In this subsection we estimate the probability of random coincidence of nine of the subionospheric signal perturbations observed on March 30, 1983, with nine of the 38 one-hop whistlers detected during the 10-min period, if the two phenomena were occurring independently.

From Figure 8 we see that the time delay between the whistler-producing spheric and the perturbation onset was 0.52–0.62 s. We then estimate the probability that nine spherics coincidentally occurred within $\sim$0.5 s of nine subionospheric perturbation events. Since the spheric occurrence was approximately a Poisson process, the probability

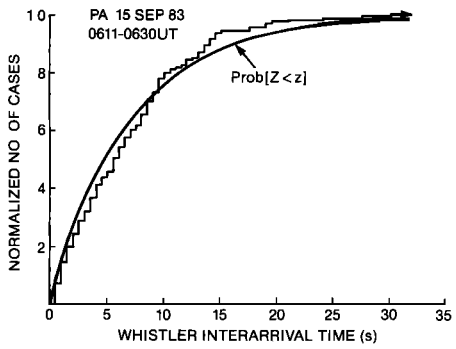

Fig. 12. Occurrence statistics of whistler-producing spherics on September 15, 1983, presented in the format of Figure 10.

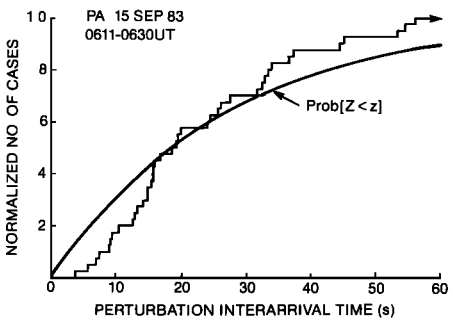

Fig. 13. Occurrence statistics of perturbations on the 37.2-kHz signal on September 15, 1983.

that at least one event occurred in a given time interval δt is [*Davenport*, 1970]

$$\text{Prob}[N_{\delta t} > 0] = 1 - e^{-\lambda \delta t} \quad (2)$$

On this basis, the probability of at least one whistler-producing spheric occurring within δt =0.5 s of one of the nine perturbation events is given by $\sim 3 \times 10^{-2}$. While this value by itself is not small enough to preclude consideration of a chance coincidence, the occurrence of coincidence on nine occasions would be of order $(3 \times 10^{-2})^9 \simeq 2 \times 10^{-14}$. We note here that although the successive occurrences of Trimpi events may not be completely independent, as noted above, the occurrence within each selected interval (however the selection is made) of a detectable whistler (regardless of its amplitude) is independent of the occurrence of whistlers in other intervals. Note also that while the delay t_d is in the range 0.52–0.62 s, the variation in delay from one event to another (Figure 8) is only $\sim$ 0.1 s. Thus one might also consider the probability that whistler-producing spherics occur within a time period δt = 0.1 s, or 0.5 $\pm$ 0.05 s after each of the nine perturbation events. This yields a probability of chance occurrence of 1.5×10^{-20}.

The above estimation inherently assumes that the occurrence of a spheric during one of the nine events does not change the probability of occurrence of another spheric during the next perturbation event. This is a good assumption when the spheric occurrence rate is higher than the perturbation occurrence rate, as it is here. However, we note that the occurrence of a spheric coincidentally with one event only reduces the probability of occurrence of another during the next perturbation, so that the probability calculated above represents an upper limit.

The probability of coincidental correlation can also be estimated for the September 15, 1983, case that was discussed in connection with Figures 12 and 13. Due to the fact that the rate of Trimpi event occurrence was twice as high during a longer observing period the estimated probability of coincidence is even lower than on March 30, being $< 10^{-36}$.

4. Precipitation Induced by a Two-Hop Whistler

Whistlers originating in southern hemisphere lightning are observed at Palmer after two-hop magnetospheric propagation, but on average are extremely rare, representing substantially less than 1% of the Palmer whistlers thus far surveyed. This rarity is attributed to a concentration of high thunderstorm activity in the northern hemisphere conjugate region and low activity within $\sim$2000 km of Palmer [e.g. *Volland et al.*, 1985]. In the March 30, 1983, broadband records, two weak two-hop whistlers were noted (none were detected on September 15). The stronger of these, occurring at the time indicated in the upper margin of Figure 2 by a star, was associated with a small amplitude perturbation on 37.2 kHz and with one of the larger changes on NPM.

Figure 14 shows expanded records of 37.2-kHz and NPM amplitude for the period of the two-hop whistler and the following one-hop whistler that was associated with event 7 in Figure 2. Spectrograms for the range 0–3 kHz are shown below; arrows mark the times of the two causative atmospherics. The first and second component of the two-hop whistler exhibit travel times that are, respectively, less than and comparable to twice the travel time of the one-hop whistlers of the period.

The precipitation effects induced by the two-hop whistler appear to have been concentrated to the west of the region affected by the one-hop events, since a relatively large change occurred on NPM on the most westerly path (event marked with a star; see also Figure 2), and no detectable changes were noted on NSS and Argentina Omega, which followed paths near the Palmer meridian (see Figure 1). The small event (event 7) produced on 37.2-kHz might have been due to weak excitation by the two-hop source of one or more of the one-hop whistler paths.

The lightning flash probably occurred near L=2 and at a distance of order 1500–2000 km from Palmer. This is qualitatively in agreement with the foregoing evidence on the spatial distribution of precipitation effects, and is supported by statistical studies of lightning [*Volland et al.*, 1985] which show a minor concentration of activity in the south eastern Pacifc. A lightning location near L = 2 is supported by the dispersion properties of the whistler noted above, and a range of $\sim$ 1500 – 2000 km is further suggested by estimates of the differential group velocity of the spheric energy near the $\sim$ 1.7-kHz cutoff frequency for the earth-ionosphere waveguide, based on the measured dispersion of the well defined spheric component.

To our knowledge this represents the first evidence of detectable electron precipitation induced by a whistler originating in the southern hemisphere. The occurrence of mixed one- and two-hop whistlers on March 30, suggests that if the sources and paths of the two type of whistlers are near the same meridian, then, in future such cases, Trimpi time signature parameters associated with both can be scaled and combined to refine physical models of the scattering process. One such model, called "mirrored precipitation," has been used to explain burst electron precipitation in the southern hemisphere induced by one-hop whistler-triggered emissions propagating outside the plasmaphause [*Rosenberg et al.*, 1971; *Helliwell et al.*, 1980] and by one-hop whistlers propagating within the plasmasphere [*Chang and Inan*, 1985]. If, as in the case of March 30, the sources and paths appear to be displaced in longitude, attention can also be paid to any corresponding differences in Trimpi activity on multiple signals, and hence to the size and distribution of precipitation regions.

5. Summary and Conclusions

We have presented case studies of whistler-associated subionospheric VLF/LF perturbations (Trimpi events) observed at Palmer, Antarctica, during two periods in 1983 for which high-time resolution broadband VLF data were available. Limited data from adjoining time periods and from several other days were also presented. The findings are generally consistent with the previously suggested cause-and-effect relationships that govern a Trimpi event, namely that the VLF/LF perturbations occur as a result of localized D region ionization enhancements caused by whistler-induced precipitation of bursts of energetic particles. In such a process involving gyroresonant particle scattering, the perturbation amplitudes would be expected to be linearly related to whistler field strength, while the temporal features would be relatively independent of event amplitude [*Chang and Inan*, 1985; *Inan et al.*, 1985].

In a case study from March 30, 1983, the perturbation amplitudes on several VLF/LF signals were indeed found to be well correlated with the associated whistler field strength.

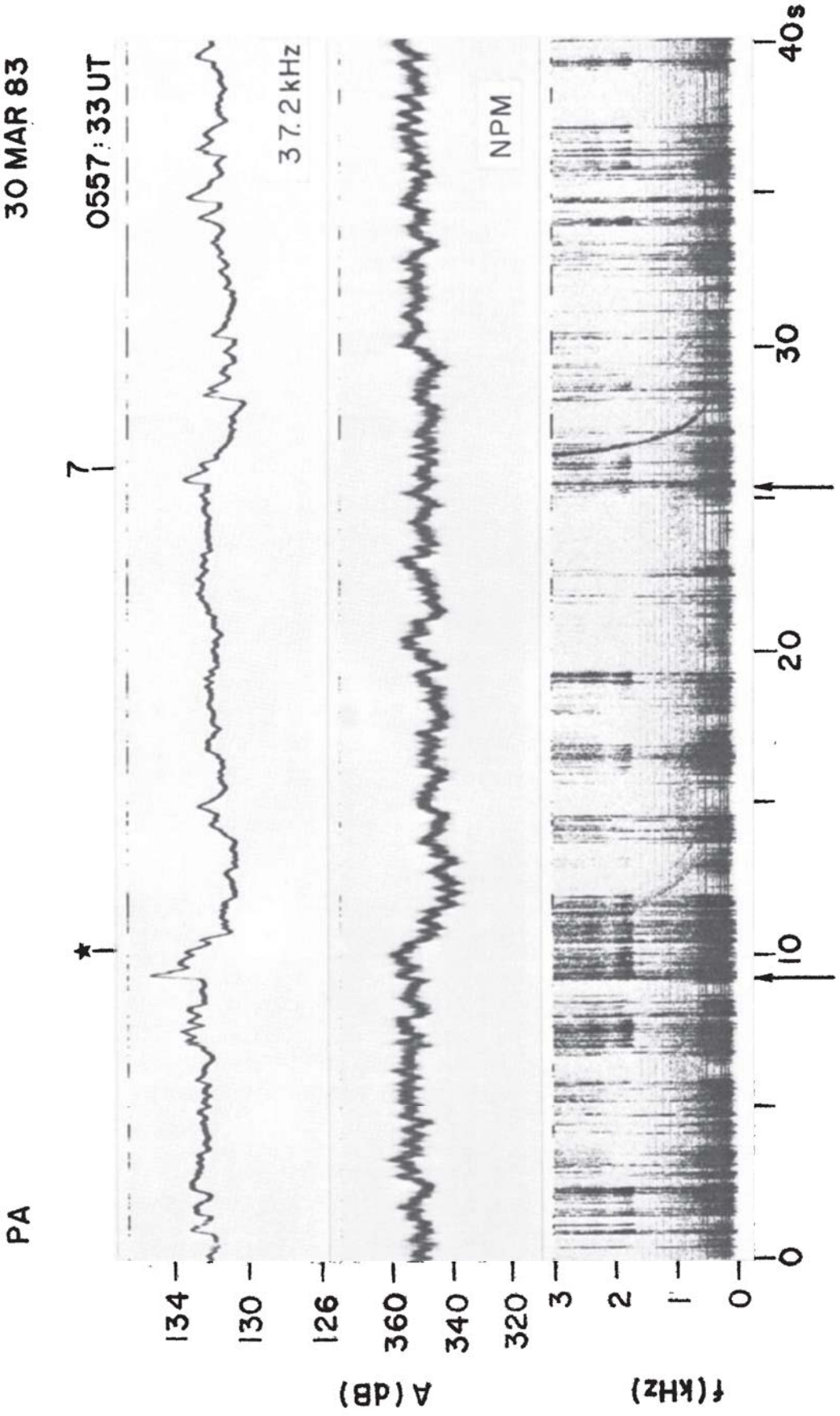

Fig. 14. Expanded records showing the perturbations marked with a star and as event 7 in Figure 2. The star is associated with a two-hop whistler triggered by southern hemisphere lightning. The upper panels show the 37.2-kHz and NPM signal amplitude, and the bottom panel shows 0- to 3-kHz frequency-time spectra. Arrows mark the causative spherics of the two hop and one-hop (event 7 in Figure 2) whistlers. The causative spheric of the two hop whistler was identified by a combination of dispersion analysis, measurements of relative spheric intensity and comparison with a second event.

On the other hand, temporal features such as a 0.52 to 0.62-s time delay between the whistler-producing spheric and the perturbation onset, as well as the rise and decay times of the perturbation, were independent of the amount of precipitation, as measured by associated whistler intensity and perturbation event amplitude. The amplitudes of simultaneous perturbations on signals of different frequency and arrival bearing were well correlated in several cases, but exhibited case to case differences that appear to depend upon the spatial distribution of precipitation regions.

Statistical analysis of whistler and signal perturbation occurrence times during two periods indicates that the probability of chance association between the whistlers and subionospheric perturbations was $< 10^{-14}$. Whistlers of all amplitudes above detection threshold were considered, and their occurrence times were found to approximately obey a Poisson distribution. However, the occurrence times of Trimpi events and of the stronger whistlers with which they were associated showed significant deviations from Poisson behavior. These deviations are probably associated with the physics of a localized region of lightning activity, which acted as a source for the stronger whistler events observed.

Although nearly all of the whistlers observed originated in northern hemisphere lightning, the first example was found of a Trimpi event associated with a southern hemisphere source. Future observations that occasionally include whistlers originating in both hemispheres sould provide additional parameters for use in probing the physics of the Trimpi effect.

Acknowledgments. We thank M. Trimpi for his work at Palmer station and J. P. Katsufrakis for his management of the Stanford field programs, and acknowledge discussions with R. A. Helliwell and other colleagues in the STAR Laboratory. We thank J. Yarbrough for production of the spectrograms, P. Pecen for her laborious efforts in carrying out the measurements and scaling of the data, and K. Fletcher for typing the manuscript. This work was supported by the Division of Polar Programs of the National Science Foundation under grants DPP-82-17820 and DPP-80-22282.

The Editor thanks A. Tolstoy and J. LaBelle for their assistance in evaluating this paper.

REFERENCES

Bailey, D. K., Some quantitative aspects of electron precipitation in and near the auroral zone, *Rev. Geophys.*, *6*(3), 1289, 1968.

Carpenter, D. L., and J. W. LaBelle, A study of whistlers correlated with bursts of electron precipitation near L=2, *J. Geophys. Res.*, *87*, 4427, 1982.

Carpenter, D. L., U. S. Inan, M. L. Trimpi, R. A. Helliwell, and J. P. Katsufrakis, Perturbations of subionospheric LF and MF signals due to whistler-induced electron precipitation bursts, *J. Geophys. Res.*, *89*, 9857, 1984.

Carpenter, D. L., U. S. Inan, E. W. Paschal, and A. J. Smith, A new VLF method for studying burst precipitation near the plasmapause, *J. Geophys. Res.*, *90*, 4383, 1985.

Chang, H. C., and U. S. Inan, A theoretical model study of observed correlations between whistler mode waves and energetic electron precipitation events in the magnetosphere, *J. Geophys. Res.*, *88*(A12), 10053, 1983.

Chang, H. C., and U. S. Inan, Lightning-induced electron precipitation from the magnetosphere, *J. Geophys. Res.*, *90*, 1531, 1985.

Davenport, W. B. Jr., *Probability and Random Processes*, McGraw-Hill, New York, 1970.

Dingle, B., Burst precipitation of energetic electrons from the magnetosphere, Ph.D. thesis, Stanford Univ. Stanford, Calif., 1977.

Dingle, B., and D. L. Carpenter, Electron precipitation induced by VLF noise bursts at the plasmapause and detected at conjugate ground stations, *J. Geophys. Res.*, *86*, 4597, 1981.

Goldberg, R. A., J. R. Barcus, L. C. Hale, and S. A. Curtis, Magnetospheric electron stimulation by lightning: Direct observation by rocket, Eos Trans. AGU, 66, 350, 1985.

Helliwell, R. A., S. B. Mende, J. H. Doolittle, W. C. Armstrong, and D. L. Carpenter, Correlations between λ4278 optical emissions and VLF wave events observed at $L \sim 4$ in the Antarctic, J. Geophys. Res., 85, 3360, 1980.

Helliwell, R. A., J. P. Katsufrakis, and M. L. Trimpi, Whistler-induced amplitude perturbation in VLF propagation, *J. Geophys. Res.*, *78*, 4679, 1973.

Hurren, P. J., and A. J. Smith, Burst precipitation-induced perturbations on multiple VLF propagation paths in Antarctica, J. Atmos. Terr. Phys., in press, 1985.

Inan, U. S., D. L. Carpenter, R. A. Helliwell, and J. P. Katsufrakis, Subionospheric VLF/LF phase perturbations produced by lightning-whistler induced particle precipitation, *J. Geophys. Res.*, *90*, 7457, 1985.

Kintner, P. M., and J. W. LaBelle, Very short path length Trimpi observations, *Eos Trans. AGU*, *65*, 1059, 1984.

Leyser, T., U. S. Inan, D. L. Carpenter, M. L. Trimpi, Diurnal variation of burst precipitation effects on subionospheric VLF/LF signal propagation near L = 2, *J. Geophys. Res.*,*89*, 9139, 1984.

Lohrey, B., and A. B. Kaiser, Whistler-induced anomalies in VLF propagation, *J. Geophys. Res.*, *84*, 5121, 1979.

Rosenberg, T. J., J. C. Siren, D. L. Matthews, K. Marthinsen, J. A. Holtet, A. Egeland, D. L. Carpenter, and R. A. Helliwell, Conjugacy of electron microbursts and VLF chorus, *J. Geophys. Res.*, *86*, 5819, 1981.

Rycroft, M. J., Enhanced energetic electron intensities at 100 km altitude and a whistler propagating through the plasmasphere, *Planet. Space Sci.*, *21*, 239, 1973.

Tolstoy, A., The influence of localized precipitation-induced D-region ionization enhancements on subionospheric VLF propagation, Ph.D. thesis, Univ. of Md., College Park, 1983.

Tolstoy, A., T. J. Rosenberg, and D. L. Carpenter, The influence of localized precipitation-induced D-region ionization enhancements on subionospheric VLF propagation, *Geophys. Res. Lett.*, *9*, 563, 1982.

Volland, H., M. Schmolders, G. W. Prölss, and J. Schäfer, VLF propagation parameters derived from sferics observations at high southern latitudes, *J. Atmos. Terr. Phys.*, in press, 1985.

Voss, H. D., W. L. Imhof, M. Walt, J. Mobilia, E. E. Gaines, J. B. Reagan, U. S. Inan, R. A. Helliwell, D. L. Carpenter, J. P. Katsufrakis, and H. C. Chang, Lightning induced electron precipitation, *Nature*, *312*, 740, 1984.

Watt, A. D., *VLF Radio Engineering*, Pergamon, New York, 1967.

D. L. Carpenter and U. S. Inan, STAR Laboratory, Stanford University, Stanford CA 94305.

(Received September 30, 1985;
revised November 15, 1985;
accepted November 18, 1985.)